Accepted Manuscript

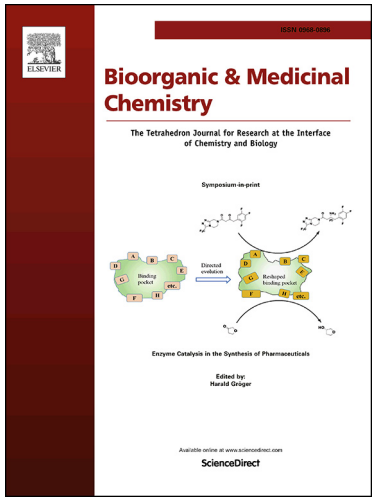

Optimization and preclinical evaluation of novel histamine H_3receptor ligands: acetyl and propionyl phenoxyalkyl piperazine derivatives

Katarzyna Szczepańska, Tadeusz Karcz, Magdalena Kotańska, Agata Siwek, Kamil J. Kuder, Gniewomir Latacz, Szczepan Mogilski, Stefanie Hagenow, Annamaria Lubelska, Michał Sobolewski, Holger Stark, Katarzyna Kieć-Kononowicz

PII: S0968-0896(18)31528-1
DOI: https://doi.org/10.1016/j.bmc.2018.11.010
Reference: BMC 14614

To appear in: *Bioorganic & Medicinal Chemistry*

Received Date: 29 August 2018
Revised Date: 26 October 2018
Accepted Date: 9 November 2018

Please cite this article as: Szczepańska, K., Karcz, T., Kotańska, M., Siwek, A., Kuder, K.J., Latacz, G., Mogilski, S., Hagenow, S., Lubelska, A., Sobolewski, M., Stark, H., Kieć-Kononowicz, K., Optimization and preclinical evaluation of novel histamine H_3receptor ligands: acetyl and propionyl phenoxyalkyl piperazine derivatives, *Bioorganic & Medicinal Chemistry* (2018), doi: https://doi.org/10.1016/j.bmc.2018.11.010

Bioorganic & Medicinal Chemistry
journal homepage: www.elsevier.com

Optimization and preclinical evaluation of novel histamine H_3 receptor ligands: acetyl and propionyl phenoxyalkyl piperazine derivatives

Katarzyna Szczepańska [a], Tadeusz Karcz [a], Magdalena Kotańska [b], Agata Siwek [c], Kamil J. Kuder [a], Gniewomir Latacz [a], Szczepan Mogilski [b], Stefanie Hagenow [d], Annamaria Lubelska [a], Michał Sobolewski [a], Holger Stark [d], Katarzyna Kieć-Kononowicz [a,*]

[a] *Department of Technology and Biotechnology of Drugs, Faculty of Pharmacy, Jagiellonian University Medical College, Medyczna 9, Kraków 30-688, Poland*
[b] *Department of Pharmacodynamics, Faculty of Pharmacy, Jagiellonian University Medical College, Medyczna 9, Kraków 30-688, Poland*
[c] *Department of Pharmacobiology, Faculty of Pharmacy, Jagiellonian University Medical College, Medyczna 9, Kraków 30-688, Poland*
[d] *Institute of Pharmaceutical and Medicinal Chemistry, Heinrich Heine University Düsseldorf , Universitaetsstr. 1, 40225 Duesseldorf, Germany*

ARTICLE INFO

Article history:
Received
Received in revised form
Accepted
Available online

Keywords:
Histamine H_3 receptor
Histamine H_3 receptor ligands
Non-imidazole histamine H_3R ligands
Piperazine derivatives
Anti-obesity agents
Molecular docking
Metabolic stability

ABSTRACT

As a continuation of our search for novel histamine H_3 receptor ligands, a series of new acetyl and propionyl phenoxyalkylamine derivatives (**2**–**25**) was synthesized. Compounds with three to four carbon atoms alkyl chain spacer, composed of six various 4N-substituted piperazine moieties were evaluated for their binding properties at human histamine H_3 receptors (hH_3R). *In vitro* test results proved the 4-pyridylpiperazine moiety as crucial element for high hH_3R affinity (hH_3R K_i = 5.2 – 115 nM). Moreover introduction of carbonyl group containing residues in the lipophilic part of molecules instead of branched alkyl substituents resulted in increased affinity in correlation to previously described series, whereas propionyl derivatives showed slightly higher affinities than those of acetyl (**16** and **22** *vs.* **4** and **10**; hH_3R K_i = 5.2 and 15.4 nM *vs*. 10.2 and 115 nM, respectively). These findings were confirmed by molecular modelling studies, demonstrating multiple ligand-receptor interactions. Furthermore, pharmacological *in vivo* test results of compound **4** clearly indicate that it may affect the amount of calories consumed, thus act as an anorectic compound. Likewise, its protective action against hyperglycemia and the development of overweight has been shown. In order to estimate drug-likeness of compound **4**, *in silico* and experimental evaluation of metabolic stability in human liver microsomes was performed.

1. Introduction

The histamine H_3 receptor (H_3R), belonging to the superfamily of G-Protein coupled receptors (GPCRs), is predominantly expressed in the central nervous system [1-3]. Since its discovery by Arrang *et al*. [4] it has been related to several central nervous system diseases by playing a key role as modulator of neurotransmitter release of e.g. dopamine, acetylcholine, noradrenaline or serotonin [1-3]. Therefore, a huge number of H_3R antagonists have been investigated on their potential therapeutic applicability in obesity, depression, mood disorders, neuropathic pain, and sleep-wake disorders (including narcolepsy) as well as cognitive and CNS-linked sensorimotor deficit disorders. Those include Parkinson's disease, attention deficit hyperactivity disorder (ADHD), Alzheimer's disease, schizophrenia, alcohol addiction, energy homeostasis, epilepsy, obstructive sleep apnea, diabetic neuropathic pain, Tourette's syndrome and catalepsy [1,5-9].

In recent years many potent and selective anti-H_3R ligands (either H_3R antagonists or inverse agonists) have been synthesized both, by academic and pharmaceutical company researchers [10-12]. From the very beginning, structures were mostly based on imidazole moiety and a number of such have found utility as pharmacological tools [13]. For this early generation of H_3R antagonists, it later appeared, that due to several possible pharmacokinetic (PK) liabilities like CYP_{450} inhibition, low brain penetration, incidence of off-target activity or lack of subtype selectivity (especially over H_4R) [6], such compounds might not serve as further clinical candidates. Therefore, the imidazole ring replacement with other heterocyclic moieties was a milestone in the search for new histamine H_3R ligands. A piperazine moiety is such a replacement, being a significant versatile scaffold in rational drug design for most of the GPCR ligands. The two secondary nitrogen atoms within the piperazine core, have an appropriate pK_a to exert the improvement in pharmacokinetic features of novel drug candidates [14]. These nitrogen sites lead to the essential increase in water solubility of the drug-like molecules, thereby playing a crucial role in bioavailability of the compounds. Maintaining the balance between pharmacodynamic and pharmacokinetic profiles

of drug-like molecules is one of the key factors in new drugs design and development. To design molecules with high affinity to their targets is one of the goals in contemporary drug discovery process. Appropriate physicochemical properties of the piperazine template makes this molecular subunit a useful and well-positioned system in the rational drug design [15].

Paying attention to the results obtained in our previous study, the 4-pyridyl-piperazino moiety has been established as a new bioisosteric piperidine replacement in H_3R ligands [16]. A position of nitrogen atom in an aromatic ring attached to piperazine moiety has turned out to be a key structural element for suitable interaction with its biological target. The most active compounds are shown in the **Figure 1**.

In order to determine the influence of substituents located in the „eastern part" of the molecule, structural modifications of previously obtained compounds including replacement of branched alkyl benzene substituents, with either acetyl or propionyl groups, were undertaken (**Figure 1**). Such carbonyl consisting moieties, present in various active compounds, e.g. Ciproxifan, might serve as additional H-bond acceptors to increase affinity at the desired target. On the other hand, our previous findings suggested that slight structural modifications involving nitrogen position change in the basic part of molecule might highly influence H_3R ligands affinity. Therefore in this study we decided to confirm these findings on structurally related compounds.

It has been shown in recent studies, that Pitolisant , an H_3R inverse agonist, might reduce body weight in obese mice [17]. To determine potential anti-obesity properties of selected compounds, preliminary pharmacological *in vivo* tests have been performed. In these studies, the influence on body weight, food and water intake, glucose and triglyceride plasma levels, and spontaneous activity on rats in the model of excessive eating of preferential feed was tested.

2. Results and discussion

2.1. Chemistry

The synthesis of desired ether derivatives **2**–**25** was achieved through the efficient synthetic route outlined in **Scheme 1**. *Para* acetyl and propionyl phenoxyalkyl bromides (**1a**–**1d**, synthesis according [18], modified by authors [16]) were obtained in one-step alkylation of *para* hydroxyaceto- and hydroxypropiophenons with α,ω-dibromoalkanes refluxed in propan-1-ol [19]. Obtained precursor bromides, after the separation from bis products emerging during synthesis, were then coupled with corresponding N-mono-substituted piperazines in the mixture of ethanol/water with powdered potassium carbonate and a catalytic amount of potassium iodide. Final products were obtained as free bases and isolated as oxalic acid salts.

2.2. Pharmacology

2.2.1. Histamine H_3 receptor affinity

All compounds in their oxalate forms were tested in H_3R *in vitro* binding studies, using slightly modified methods to those described previously [20]. Briefly, compounds were tested at five to eleven appropriate concentrations in a [^{3}H]N^{α}-methylhistamine (K_D = 3.08 nM) radioligand depletion assay to determine the affinity at human recombinant histamine H_3R stably expressed in HEK-293 cells.

In vitro affinity data are assembled in **Table 1**. According to our assumptions, 4-pyridyl derivatives **4**, **10**, **16** and **22** showed the highest affinity among tested compounds, much higher than in our previous study (with exception of compound **10** *vs.* previously described *t*-butyl analogue; hH_3R K_i = 115 nM *vs.* 37.8 nM respectively), indicating the importance of lipophilic part involvement in interaction with the H_3R binding site. Among 4-pyridyl derivatives, compound **16** (hH_3R K_i = 5.2 nM) is the most active one described in this work. In this subgroup of compounds, affinities tend to be higher for propionyl compared to acetyl derivatives (**16** and **22** *vs.* **4** and **10**; hH_3R K_i = 5.2 and 15.4 nM *vs.* 10.2 and 115 nM, respectively), however, lacking statistical significance.

3-Pyridyl piperazine derivatives appear to be similarity active than 2-pyridyl derivatives, with the exception of compounds **8** *vs.* **9**, where 3-pyridyl derivative **9** was three orders of magnitude more potent than its 2-pyridyl analogue **8**. Moreover, in case of dihetero aromatic substituents, no significant difference in antagonistic properties between 2-(1-piperazinyl)pyrazine and 2-piperazinopyrimidine derivatives was observed. Comparable to our previous results, tetrahydrofuroyl derivatives (**7**, **13**, **19**, **25**) showed no H_3R affinity.

Paying attention to the alkyl linker length, derivatives with a four methylene linker tend to be less active than their three methylene homologues, with the exception of compounds **5** *vs.* **11** and **6** *vs.* **12** (hH_3R K_i = 2316 *vs.* 1230 nM and 2453 *vs.* 1634 nM, respectively).

2.2.2. Locomotor activity

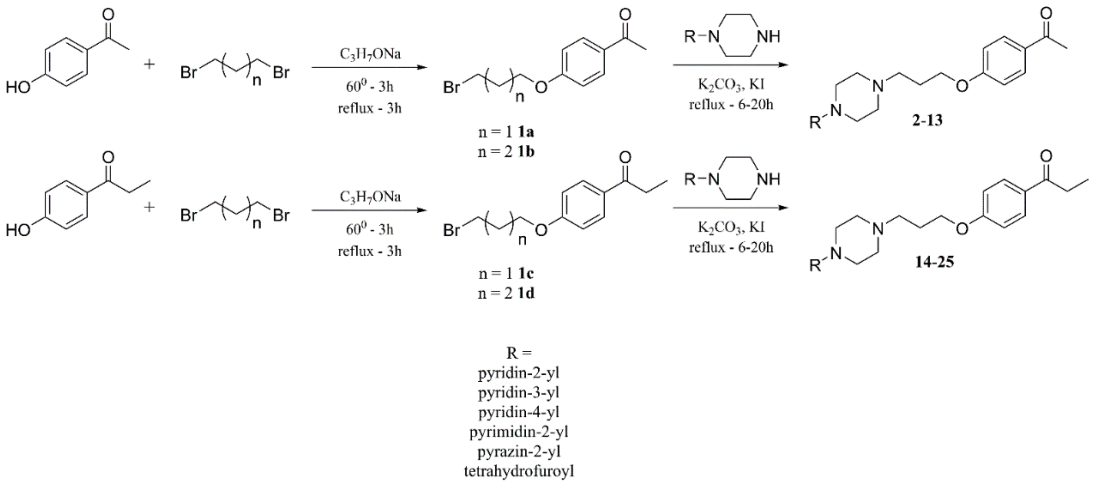

Scheme 1. General synthetic pathway for compounds **2**–**25**.

Table 1.
Structures of compounds **2**–**25** and their *in vitro* histamine H_3 receptor (hH_3R) affinities. Given data represent mean values within the 95% confidence interval (CI).

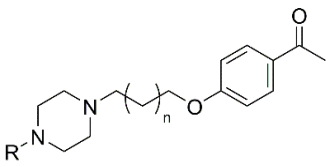

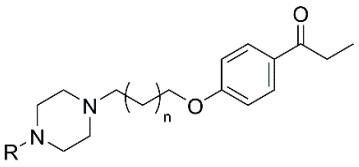

No.	n	R	hH_3R K_i [nM] $\bar{x}$ [CI 95%]	No.	n	R	hH_3R K_i [nM] $\bar{x}$ [CI 95%]
2	1	pyridin-2-yl	315 [132, 754]	**14**	1	pyridin-2-yl	377 [116, 1226]
3	1	pyridin-3-yl	499 [261, 953]	**15**	1	pyridin-3-yl	192 [42.4, 871]
4	1	pyridin-4-yl	10.2 [3.6, 29.0]	**16**	1	pyridin-4-yl	5.2 [0.7, 41.5]
5	1	pyrazin-2-yl	2316 [940, 5707]	**17**	1	pyrazin-2-yl	3390 [1528, 7521]
6	1	pyrimidin-2-yl	2453 [461, 13047]	**18**	1	pyrimidin-2-yl	1720 [802, 3687]
7	1	tetrahydrofuroyl	4889 [800, 29862]	**19**	1	tetrahydrofuroyl	1392 [470, 4128]
8	2	pyridin-2-yl	3697 [2563, 5332]	**20**	2	pyridin-2-yl	1444 [172, 12101]
9	2	pyridin-3-yl	908 [230, 3582]	**21**	2	pyridin-3-yl	1392 [264, 7346]
10	2	pyridin-4-yl	115 [26.8, 493]	**22**	2	pyridin-4-yl	15.4 [0.6, 429]
11	2	pyrazin-2-yl	1230 [377, 4021]	**23**	2	pyrazin-2-yl	4040 [1099, 14850]
12	2	pyrimidin-2-yl	1634 [619, 4318]	**24**	2	pyrimidin-2-yl	3627 [736, 17879]
13	2	tetrahydrofuroyl	> 10000	**25**	2	tetrahydrofuroyl	> 10000

In order to determine the influence on locomotor activity, compounds were tested in two doses 3 and 5 mg/kg b.w. The results showed that single administration of compounds **4** and **16** (5 mg/kg b.w., *i.p.*) caused a significant decrease in locomotor activity when compared to vehicle-treated animals (**Figure 2**). However, there were no significant changes in activity at dose of 3 mg/kg b.w. Disorders of spontaneous activity (significant increase in activity as well as sedation) induced by the test compound could disturb the assessment of the test compound impact on body weight. Therefore, a dose of 3 mg/kg b.w. for chronic tests was chosen.

2.2.3. Body weight and food intake in rats fed with palatable diet

The animals fed with palatable feed and receiving compound **4** (3 mg/kg b.w. per day) showed significantly less weight gain than rats from the control group consuming a preferential feed. From the 9th day of the experiment, a statistically significant difference in body weight between the groups was observed (e.g. day 9 with 8.64% *vs.* day 14 with 7.89%). Most importantly, the body weight of rats with access to preferential feed and treated with compound **4** treatment, did not differ significantly from that of the control group fed with a standard feed (**Figure 3A**). There was no significant decrease in weight gain when compound **4** was administrated at dose 1 mg/kg b.w./day. The weight of these animals grew in a similar manner to animals consuming preferential feed and receiving a vehicle.

Compared to control group consuming a preferential feed, the rats fed with palatable feed and treated with compound **16** (3 mg/kg b.w. per day) showed no significant changes in weight gain. Animals from the test group gained weight similarly to animals from the control group during the experiment (**Figure 3B**).

Compound **4** administered intraperitoneally at the dose of 3 mg/kg b.w. per day significantly reduced the amount of consumed calories by the animals on a palatable diet in comparison to the ones of the control group (**Figure 4**).

Compound **4** acts much better in conducted research, although both compounds are characterized by similar affinities to H_3R. Their kinetics, absorption, biotransformation, half-life, metabolism etc. might indeed play important role. However H_3R besides its presynaptic auto- and heteroreceptor activity in the central nervous system, is active in peripheral tissues, e.g. adipocytes and the capillary network in brown adipose tissue [21]. Therefore, further studies are needed to elucidate the mechanism of both compounds action in this regard.

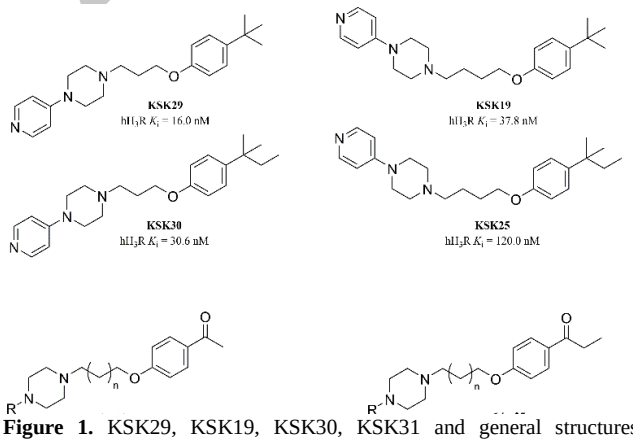

Figure 1. KSK29, KSK19, KSK30, KSK31 and general structures of described ligands **2**–**25**; hH_3R – human histamine H_3 receptor.

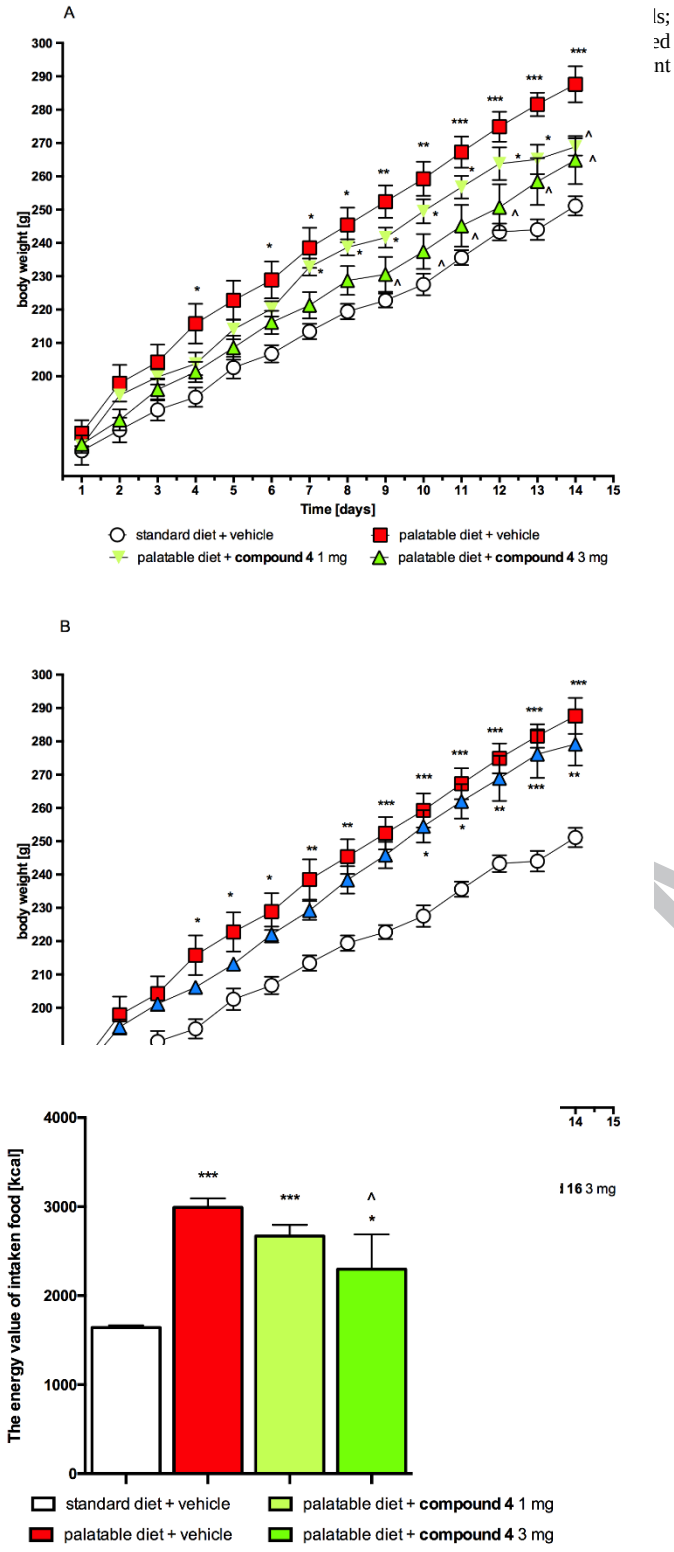

Figure 4. The energy value of intaken food during administration of compound **4**. Results are expressed by mean ± SEM, n = 6. Multiple comparisons were performed by two-way ANOVA, Bonferroni post-hoc or one-way ANOVA Tukey post-hoc. *p < 0.05, **p < 0.01, ***p < 0.001 significant between control rats fed with palatable diet *vs.* control rats fed with standard diet; ^p < 0.05 significant between control rats fed with palatable diet *vs.* rats treated with tested compounds.

Figure 3. Effect of administration of tested compounds on body weight. A) Body weight throughout the administration of compound **4**. B) Body weight throughout the administration of compound **16**. Multiple comparisons were performed by two-way ANOVA, Bonferroni post-hoc or one-way ANOVA Tukey post-hoc. *p < 0.05, **p < 0.01, ***p < 0.001 significant between control rats fed with palatable diet *vs.* control rats fed with standard diet; ^p < 0.05 significant between control rats fed with palatable diet *vs.* rats treated with tested compounds.

triglyceride and glucose level

The level of glucose and triglyceride in blood was higher in rats on the palatable *vs.* standard diet. Rats treated with compound **4** for two weeks and fed with a palatable diet had significantly lower level of glucose in plasma in comparison to the control group fed with the palatable diet (**Figure 5A**). On the other hand, no significant effect on triglyceride level of rats fed with palatable diet was observed in comparison with the control group. Interestingly, the group that received compound **4**, had significantly lower amount of fat in the peritonea compared to the obese rats (**Figure 5B**).

It can be assumed that decreased glucose level may be directly related to weight loss. However, our research was of a preliminary character and did not indicate the mechanism of this action. It might be possible that this compound affects the secretion of insulin. As it was shown earlier by Nakamura et al. [22], histamine H_3 receptors are expressed in mouse β cells and could play a role in insulin secretion and possibly β cell proliferation. Histamine H_3 receptor inverse agonist Pitolisant administrated for 14 days in obese mice significantly improved glucose tolerance [17]. Other inverse agonist JNJ-5207852 induces insulin secretion from pancreatic β cells and corrects glucose level [22]. Further studies are needed to elucidate the mechanism of tested compounds action in this regard.

2.2.5. Spontaneous activity in chronic dosing

The group chronically treated with compound **4** showed no significant differences in spontaneous activity compared to rats fed only with palatable feed (**Figure 6**). Disorders of spontaneous activity (significant increase in activity as well as sedation) and the stress induced by the test compound could be very disadvantageous and could disturb an impact assessment of the test compound on body weight [23]. The test compound **4** did not cause sedation or hyperlocomotion. Therefore, the observed anorectic effect was definitely not associated with a reduction or increment in the spontaneous activity of animals.

2.3. Metabolic stability

The metabolic stability of compound **4** was initially examined using MetaSite computational tool in order to determine the potential sites of metabolism as well as structures of potential metabolites [24]. Prediction results of **4** by a computational liver model, and *in vitro* metabolic stability studies using human (HLMs) liver microsomes are given in Supplementary Data.

In silico data indicated the nitrogen atom of the pyridine moiety as the most probable site of compound **4** metabolism. Moreover, the aliphatic linker and the methyl group at acetyl substituent were also shown to be susceptible for metabolic biotransformations. The provided *in silico* the most likely structures of compound **4** metabolites showed that the metabolic oxidation/hydroxylation are expected, which occurred either at nitrogen of the pyridine moiety or at the methyl group of acetyl substituent (see Supplementary Data).

In vitro test results suggested very good metabolic stability of compound **4**, as only ~9% was converted into two metabolites. In MS analysis, the observed molecular masses and ion fragments of **4**, as well as its main metabolite **M1** (+2 units) and **M2** (+16 units) suggest the reduction of the carbonyl group and the reaction of oxidation/hydroxylation as metabolic routes of compound **4**. Surprisingly, the determined *in vitro* reduction of the carbonyl group in **M1** was in opposite to the *in silico* results. However, two oxidized or hydroxyled metabolites with molecular masses similar to obtained *in vitro* **M2** were predicted by MetaSite software. The site of **M2** metabolic

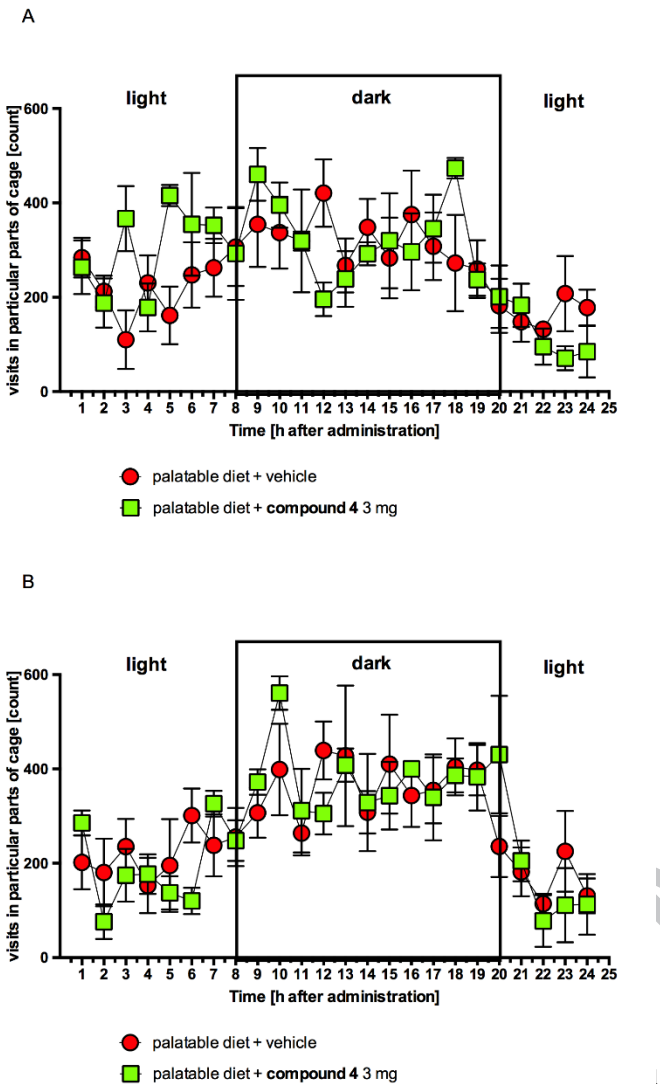

plasma triglyceride level in rats (A) and the amount of peritoneal fat in rats

Figure 6. Spontaneous activity after first (A) and thirteenth (B) administration of compound **4**. Results are expressed by mean ± SEM, n=6. Comparisons were performed by Multiple t-test.
standard diet; ^p < 0.05, ^^p < 0.01 significant between control rats fed with palatable diet *vs.* rats treated with compound **4**.

biotransformation was determined next due to the fragment ion with *m/z* = 176 produced by **M2**, which excluded the *N*-oxidation at the pyridine moiety. Thus, considering both *in silico* and *in vitro* results the metabolite **M2** of compound **4** is a hydroxyl derivative with hydroxyl group located most likely at the methyl group of acetyl substituent (see Supplementary Data).

2.4. Hepatotoxicity – the effect on HepG2 cells

The potential antiproliferative activity of **4** was examined *in vitro* by using hepatoma HepG2 cells to predict its potential hepatotoxicity. The statistically significant decrease in the cells viability was observed at 10 µM ($p < 0.01$) and 100 µM ($p < 0.001$) concentrations. However, the effect was weak (~10% decrease in HepG2 viability), compared to the reference toxins CCCP and DX, which decreased more than 50% of control HepG2 viability at 10 µM and 1 µM, respectively (**Figure 7**).

2.5. Risk for Phospholipidosis

Many of the marketed cationic amphiphilic drugs (CADs) are responsible for side effects connected with a lysosomal accumulation of phospholipids (phospholipidosis, PLD). The CADs are characterized by a hydrophobic ring structure and a hydrophilic side chain with a charged amine group. The CADs-induced PLD is associated with number of unwanted clinical toxicities, such as hepatotoxicity, QT prolongation, kidney and lung injury, and myopathy [25].

During this study the LYSO-ID Red Detection Kit (Enzo, Farmingdale, NY, USA) was used for prediction of potential PLD effect induced by compound **4** in HepG2 cells. The used kit consists of the LYSO-ID Red fluorescent dye, which accumulates in lysosomes, and Hoechst 33342 nuclear stain. HepG2 cells were treated for 72h with the reference PLD-inducing drugs Verapamil, Ketoconazole and tested compound **4** at a concentration of 50 µM. Next, the compounds were removed and the cells were incubated for 30 min with the mixture of LYSO-ID Red and Hoechst 33342 and analyzed by fluorescence microscopy. The reference drugs considerably increased the number of cellular lysosomes in hepatoma cells in comparison to the untreated control. However, much lower number of lysosomes were observed for compound **4** (see Supplementary Data).

2.6. Molecular modeling

Among four known and described histamine receptors, only the histamine H_1 receptor crystal structure was resolved so far (PDB ID: 3RZE [26]). Therefore, in search for novel histamine H_3 receptor ligands, homology modeling methods are used for the H_3R binding site. In this study, for docking purposes, previously described histamine H_3 receptor homology model was used (with Pitolisant as reference ligand in the binding pocket [16]).

All of the docked compounds were characterized by relatively high docking score values between -8.391 and -5.11. Both the highest and lowest values were observed for *p*-acetyl derivatives. Supposed key histamine H_3 receptor antagonist/inverse agonist interactions are salt bridge and/or hydrogen bond formation between protonated piperazine nitrogen and GLU206$^{5.46}$ (upper case numeration according to Balesteros-Weinstein [27]) for most of the compounds.

Similar to our previous findings, H-bond formation between TYR374$^{6.51}$ and ether oxygen was observed for compounds with alkyl chain composed of 4-methylene groups. Additionally, heteroaromatic substituents at the terminal nitrogen were stabilized through π-π interactions with indole and/or benzene ring of TRP 371$^{6.48}$ (**Figure 8**), one of the highly conserved residues, so-called molecular switches [28], for which the change of orientation causes a change in the conformation of the receptor. Again, due to the electron structure of tetrahydrofuroyl moiety, such interactions were not observed for those piperazine substituents.

Figure 7. The effect of compound **4** and the reference toxins DX and CCCP on the hepatoma HepG2 cells viability. The statistical significance was evaluated by a one-way ANOVA, followed by Bonferroni's Comparison Test (**p < 0.01, ***p < 0.001 compared with negative control).

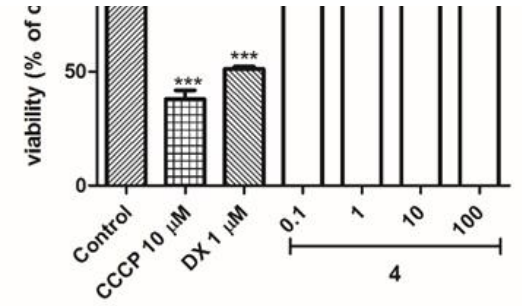

Substituted benzene rings in the lipophilic part of ligands were stabilized through π-π stacking with at least one of aminoacids TYR 115$^{3.33}$, TYR 394$^{7.35}$, PHE 193 (ECL2). For most of the compounds, additional formation of a hydrogen bond between carbonyl group and ARG381$^{6.58}$ nitrogens was found. These interactions might have a positive influence on H_3R affinity for the set of tested ligands, in comparison to previously described *t*-amyl and *t*-butyl derivatives. Although, with the elongation of the alkyl chain length, the position of basic parts of the ligands was mostly fixed, acetyl and propionyl substituents reached progressively higher in the extracellular direction. In most cases this led to loss of π-π stacking stabilization and/or H-bond with TYR374$^{6.51}$, yet still maintaining its interactions with ARG381$^{6.58}$ (**Figure 9**).

3. Conclusions

A novel series of acetyl and propionyl phenoxyalkylamine derivatives investigated proved to be potent histamine H_3R ligands with some compounds with the H_3R affinities in the nanomolar concentration range. *In vitro* test results proved the 4-pyridylpiperazine moiety to be a crucial element for high hH_3R affinity (hH_3R K_i = 5.2 – 115 nM). Moreover, introduction of carbonyl moiety containing residues in the lipophilic part of molecules instead of branched alkyl substituents resulted in increased affinity. This is in accordance with our previously described series, whereas propionyl derivatives showed slightly higher affinities compared to those of acetyl derivatives (**16** and **22** vs. **4** and **10**; hH_3R K_i = 5.2 and 15.4 nM to 10.2 and 115 nM, respectively). These findings were confirmed by molecular modelling studies, where additional ligand-receptor interactions were found. Yet again, dinitrogen piperazine substituents showed significantly lower affinity and tethrahydrofuroyl were completely inactive.

Pharmacological *in vivo* test results of compound **4** (3 mg/kg) clearly indicate that it may affect the amount of calories consumed, thus act as an anorectic compound. Likewise, its protective action against hyperglycemia and the development of overweight has been shown. In the effective dose, compound **4** did neither affect the activity, nor acted seditiously. Moreover, studies of **4** showed its safety and very good metabolic stability. Thus, compound **4** has been chosen as a new lead structure for development of anti-obese H_3R ligands and the mechanism of its action would be a subject of further studies.

4. Experimental protocols

4.1. Chemistry

All reagents were purchased from commercial suppliers and were used without further purification. Melting points (m.p.) were determined on a MEL-TEMP melting point apparatus II (LD Inc., USA) and are uncorrected. Mass spectra (LC/MS) were performed on Waters TQ Detector mass spectrometer. ^{1}H NMR spectra were recorded on a Varian Mercury 300 MHz PFG spectrometer in DMSO-d_6. Chemical shifts were expressed in parts per million (ppm) using the solvent signal as an internal standard. Data are reported in the following order: multiplicity (s, singlet; d, dublet; t, triplet; qi, quintet; m, multiplet; br, broad; Ac, acetyl; Prop, propionyl; Ph, phenyl; Pip, piperazine; Pyr, pyridine; Pym, pyrimidine; Pyz, pyrazine; Thf, tetrahydrofuran), approximate coupling constants *J* expressed in Hertz (Hz), number of protons. ^{13}C NMR spectra were recorded on Varian-Mercury-VX 300 MHz PFG or Brukker 400 MHz spectrometer at 75 MHz in DMSO-d_6. LC–MS were carried out on a system consisting of a Waters Acquity UPLC, coupled to a Waters TQD mass spectrometer. Retention times (t_R) are given in minutes. Elemental analyses (C, H, N) were performed on an Elemental AnalyserVario El III (Hanau, Germany). For CC purification (column chromatography using silica gel 60 (0.063–0.20 mm; Merck) solvent systems were used: I: petroleum ether:EtOAc (9:1); II: CH_2Cl_2:MeOH (9:1).

*4.1.1. General synthetic procedure for compounds **1a**–**1d***

To a solution of freshly prepared sodium propanolate, proper substituted phenols were added and stirred at room temperature for 5 min. α,ω-dibromoalkanes were then added dropwise in the time of 1 h. The reaction mixture was stirred at 60°C for 3 h, and then refluxed for another 3 h. After cooling down to RT, mixture was filtrated and evaporated. To a rough product, 100 ml of 10%

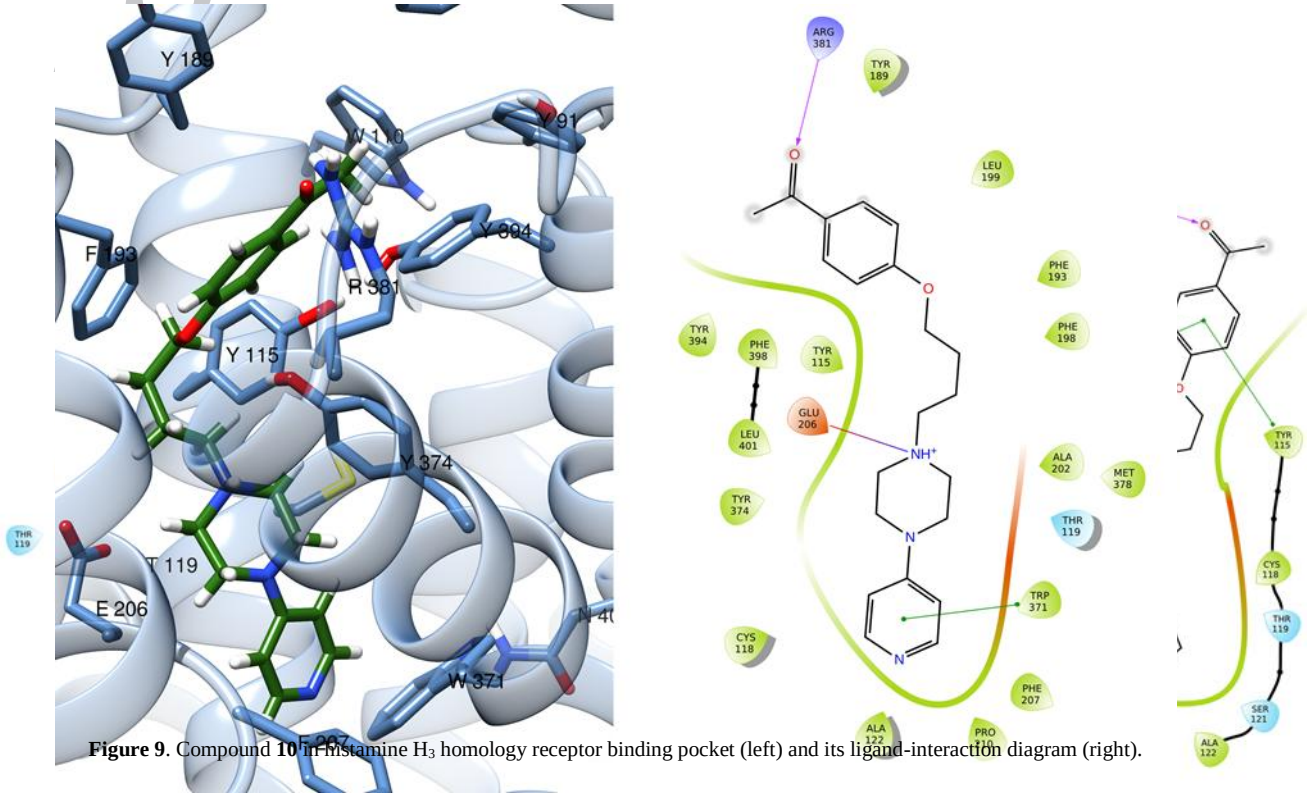

Figure 9. Compound **10** in histamine H_3 homology receptor binding pocket (left) and its ligand-interaction diagram (right).

NaOH was added and left overnight in cold. To a resulting white oil CH_2Cl_2 was added, mixed and layers were then separated. Organic layer was dried over sodium sulphate, filtered and evaporated. Resulting product was used for further reactions after CC purification.

*4.1.1.1. 1-(4-(3-Bromopropoxy)phenyl)ethan-1-one (**1a**)*

Synthesis from 1-(4-hydroxyphenyl)ethan-1-one (13.62 g, 0.1 mol), 1,3-dibromopropane (40.38 g, 0.2 mol) in sodium propanolate (0.1 mol, 100 ml). 18.51 g of raw product was obtained, purified by CC (I) with yield of 72%.

*4.1.1.2. 1-(4-(4-Bromobutoxy)phenyl)ethan-1-one (**1b**)*

Synthesis from 1-(4-hydroxyphenyl)ethan-1-one (13.62 g, 0.1 mol), 1,4-dibromobutane (43.18 g, 0.2 mol) in sodium propanolate (0.1 mol, 100 ml). 19.25 g of raw product was obtained, purified by CC (I) with yield 71%.

*4.1.1.3. 1-(4-(3-Bromopropoxy)phenyl)propan-1-one (**1c**)*

Synthesis from 1-(4-hydroxyphenyl)propan-1-one (15.02 g, 0.1 mol), 1,3-dibromopropane (40.38 g, 0.2 mol) in sodium propanolate (0.1 mol, 100 ml). 18.43 g of raw product was obtained, purified by CC (I) with yield 68%.

*4.1.1.4. 1-(4-(4-Bromobutoxy)phenyl)propan-1-one (**1d**)*

Synthesis from 1-(4-hydroxyphenyl)propan-1-one (15.02 g, 0.1 mol), 1,4-dibromobutane (43.18 g, 0.2 mol) in sodium propanolate (0.1 mol, 100 ml). 17.68 g of raw product was obtained, purified by CC (I) with yield 62%.

*4.1.2. General synthetic procedure for compounds **2**–**25***

To a suspension of potassium carbonate and catalytic amount of potassium iodide in water, a mixture of proper cyclic amine and compound **1a**–**1d** in ethanol was added. Mixture was then refluxed for 8–20 h (TLC controlled). After cooling down to room temperature, reaction mixture was filtrated, evaporated and purified. To a resulting oil, 100 ml of CH_2Cl_2 was added and washed with: 0.5% HCl solution, 0.5% NaOH solution and water. After drying over anhydrous Na_2SO_4 and evaporation of organic layer product was further purified using CC (II).

Detailed synthetic procedure and analytical data for compounds **2**–**25** could be found in Supplementary Data.

*4.1.2.1. 1-(4-(3-(4-(Pyridin-2-yl)piperazin-1-yl)propoxy)phenyl)ethan-1-one hydrogen oxalate (**2**)*

Synthesis from 1-(pyridin-2-yl)piperazine (0.82 g, 5 mmol), and compound **1a** (1.29 g, 5 mmol) in ethanol (50 ml) in the presence of K_2CO_3 (1.17 g, 8.5 mmol) and catalytic amount KI in water (10 ml). Reaction was refluxed for 20 h and then purified. Obtained 1.44 g of oil with yield of 72%. Raw product was transformed into oxalic acid salt yielding 0.88 g of final compound. Mp: 182–183 °C. ^{1}H NMR (300 MHz, DMSO-d_6) δ ppm: 8.13 (dd, J=4.69, 1.17 Hz, 1H, 2Pyr-6H), 7.91 (m, J=8.79 Hz, 2H, Ph-3,5H), 7.57 (ddd, J=8.79, 7.03, 1.76 Hz, 1H, 2Pyr-4H), 7.03 (m, J=8.79 Hz, 2H, Ph-2,6H), 6.90 (d, J=8.21 Hz, 1H, 2Pyr-3H), 6.70 (dd, J=6.74, 4.98 Hz, 1H, 2Pyr-5H), 4.13 (t, J=5.86 Hz, 2H, CH_2-O), 3.70 (br. s., 4H, Pip-3,5H), 3.04-3.15 (m, 6H, Pip-2,6H + NCH_2), 2.50 (s, 3H, CO-CH_3), 2.07-2.18 (m, 2H, CH_2-CH_2-O). ^{13}C NMR (DMSO-d_6): 196.74, 164.52, 162.63, 158.69, 148.03, 138.26, 130.93, 130.45, 114.73, 114.30, 108.00, 66.00, 53.73, 51.47, 42.98, 26.87, 24.36. LC–MS: purity 100% t_R = 2.72, (ESI) m/z $[M+H]^+$ 341.33. Anal. Calcd for $C_{20}H_{25}N_3O_2$ x $C_2H_2O_4$: C, 61.53, N, 9.78, H, 6.34%. Found: C, 60.95, N, 9.82, H, 6.28.

4.2. Pharmacology

4.2.1. [^{3}H]N^α-Methylhistamine hH_3R displacement assay

Competition binding data were analyzed using GraphPadPrism (V6.01, San Diego, CA, USA) software, using non-linear least squares/regression fit. K_i values were calculated from IC_{50} values according to Cheng-Prusoff equation [29]. Affinity values (K_i) were expressed as mean (with 95% confidence interval) from at least three experiments, each performed at least in duplicates.

The displacement binding assay was carried out as described by Kottke et al. with slight modifications [20]. Frozen crude membrane preparations of HEK-293 cells stably expressing the recombinant hH_3R in full length were thawed, homogenized, incubated for 90 min at RT (continuous shaking) with [^{3}H]N^α-methylhistamine (2 nM) and different concentrations of the test compounds (five to eleven appropriate concentrations between 0.01 nM and 10 µM were used) in a final assay volume of 200 µl per well. Non-specific binding was determined in the presence of Pitolisant (10 µM). The bound radioligand was separated from free radioligand by filtration through GF/B filters (pretreated with 0.3% (m/v) polyethyleneimine) using an Inotech cell harvester (Dottikin, Switzerland). Unbound radioligand was removed by three washing steps with 0.3 ml/well of ice-cold water. Scintillation cocktail was added and the liquid scintillation counting was performed with a Perkin Elmer TriluxBeta counter (Perkin Elmer, Germany).

4.2.2. In vivo studies

4.2.2.1. Drugs and compounds

Heparin was delivered by Polfa Warszawa S.A. (Warsaw, Poland), while thiopental sodium was from Sandoz International (France).

4.2.2.2. Animals

The experiments were carried out on male CD-1 mice, body weight 20 - 22 g (locomotor activity) or Wistar rats, initial body weight 160 - 180 g (body weight, biochemical assays, spontaneous activity). Animals were housed in pairs in plastic cages in constant temperature facilities exposed to light-dark cycle, water and food available *ad libitum*. Control and experimental groups consisted of six to eight animals each. All experiments were conducted according to the Guidelines of the Animal Use and Care Committee of the Jagiellonian University.

4.2.2.3. The influence of test compounds on locomotor activity

The locomotor activity was recorded with an Opto M3 multichannel activity monitor (MultiDevice Software v1.3, Columbus Instruments, USA). Locomotor activity was evaluated as the distance travelled by the animals while attempting to climb upward [30]. Mice were inserted into the parameter-counting cage immediately after the intraperitoneal administration of the test compound, although the activity measurement started 30 minutes after administration of the test compound over a 20 minutes period.

4.2.2.4. The influence of test compounds on body weight and food and water intake in rats fed with palatable diet (Western-style diet)

In order to determine the anorectic activity of compounds, its effect on calories and water intake in the model of excessive eating was assessed [31]. Four groups composed of six rats were fed during two weeks with a diet consisting of milk chocolate with nuts, cheese, salted peanuts and 7% condensed milk.

Animals had access to standard food (Labofeed B, Morawski Manufacturer Feed, Poland) and water *ad libitum*. Rats were treated intraperitoneally with compounds once a day in the morning for 14 days. The palatable control group received a vehicle intraperitoneally (1% Tween 80) whereas test palatable groups received: 3 mg/kg b.w. of compound **16** or 3 mg/kg b.w. of compound **4** or 1 mg/kg b.w. of compound **4** in 1% Tween 80. Palatable diet contained: 100 g peanuts – 614 kcal; 100 ml condensed milk – 131 kcal; 100 g milk chocolate with hazelnuts – 195 kcal; 100 g Greek cheese – 270 kcal. The other group of rats was on a standard diet (100 g feed – 280 kcal). A vehicle (1% Tween 80) was administered intraperitoneally to this control group. The consumption of food and water was evaluated three times per week and body weight of animals was measured daily, immediately before administration of substances. On the 15th day of the experiment, 20 minutes after intraperitoneal administration of heparin (1000 j/rat) and thiopental (70 mg/kg b.w.), plasma was collected from the left carotid artery and peritoneal fat was weighed.

*4.2.2.5. Influence of compound **4** on glucose and triglyceride levels*

To determine the glucose and triglyceride levels in plasma, standard enzymatic and spectrophotometric tests (Biomaxima S.A. Lublin, Poland) were carried out [17]. The substrate was decomposed with enzymes suitable to the relevant product, which was then converted to a colored compound. The coloration was proportional to the concentration. The absorbance was measured at a wavelength of 500 nm (glucose, triglycerides).

*4.2.2.6. Influence of compound **4** on spontaneous activity after chronic treatment in rats fed palatable diet housed in pairs in home cages*

The spontaneous activity of rats treated with compounds was measured on the 1st and 13th day of the treatment using special RFID-system – TraffiCage (TSE-Systems, Germany). Rats were housed in pairs in domestic cages with feed and water available *ad libitum*. The animals had transmitter identification (RFID) implanted subcutaneously, which enabled to count the presence and time spent in different areas of the cage, and then to collect the data with special computer application. Spontaneous activity was monitored for 24 hours after administration of the compound.

4.2.2.7. Statistical analysis

Statistical calculations were carried out with the GraphPad Prism 6 [32] program. Results are given as the arithmetic means with standard error of the mean (SEM). Statistical significance was calculated using one of the following tests: two-way ANOVA post-hoc Bonferroni test (body weight changes); one-way variance analysis (ANOVA), followed by a Dunnett post-hoc test (triglyceride and glucose levels, energy intake); t-Student test (locomotor activity); Multiple t-test, under the assumption, that all of the rows were sampled from populations with the same scatter (spontaneous activity). Differences were considered statistically significant at: $*p \leq 0.05$, $**p \leq 0.01$, $***p \leq 0.001$.

4.3. Metabolic stability

In silico investigation was performed by MetaSite 6.0.1 provided by Molecular Discovery Ltd. The most probable sites of metabolism were predicted during this study by liver computational model [24]. Human liver microsomes (HLMs) for *in vitro* metabolic stability determination were purchased from Sigma-Aldrich (St. Louis, MO, USA). The NADPH Regeneration System was purchased from Promega (Madison, WI, USA). All experiments were performed as described before [32,33]. Mass spectra were recorded on LC/MS system consisted of a Waters Acquity UPLC, coupled to a Waters TQD mass spectrometer (electro spray ionization mode ESI-tandem quadrupole).

4.4. Antiproliferative assay

Hepatoma HepG2 (ATCC HB-8065) cell line was kindly donated by the Department of Pharmacological Screening, Jagiellonian University Medical College. The cell cultures' growth conditions were applied as described before [33,34]. The cytostatic drug doxorubicin (Sigma-Aldrich) and hepatotoxin - carbonyl cyanide 3-chlorophenylhydrazone, CCCP (Sigma-Aldrich) were used as references. CellTiter 96 AQueous Non-Radioactive Cell Proliferation Assay (MTS) (Promega) was used to determine cells' viability. The absorbance of the samples was measured using a microplate reader EnSpire (PerkinElmer) at 490 nm.

4.5. Phospholipidosis

To determine the drug-induced phospholipidosis the HepG2 cells were seeded first in 96-wells white, solid plate with transparent bottom (Corning, Tewksbury, MA, USA) at concentration of 1.5×10^4 cells/well and were incubated at 37°C for 24 hours in a humidified atmosphere at 5% CO_2. Next, Verapamil, Ketoconazole and compound **4** were diluted in glucose (4.5 g/L) and FBS (10%) supplemented Minimum Essential Medium Eagle (MEM) media (Gibco, Carlsbad, CA, USA) and added to the cells in the concentration of 50 µM. The cells were incubated for 72 h. Thereafter, the medium with compounds was removed and the cells were incubated for 30 min with the mixture of LYSO-ID Red and Hoechst 33342 (Enzo, Farmingdale, NY, USA). The cells were next washed twice with 200 µl of PBS Buffer and analyzed by fluorescence microscopy DMi8 (Leica, Wetzlar, Germany).

4.6. Molecular modeling

For docking purposes, Schrödinger Maestro Suite (v. 11.5.011, Release 2018-01) was used [35]. Ligands were built in their ionized forms (protonated N4 piperazine nitrogen, structure charge +1) and their bioactive conformations were generated using ConfGen module [36,37] (water environment, target number of conformers – 20). Binding site was centered on ligand placed in homology model (Pitolisant). Docking to rigid form of receptor was performed using Glide module [38-42] (precision standard, flexible ligand sampling, max 5 poses per conformer). Ligands were rated according their position in binding pocket, interactions with binding pocket amino acids, as well as the docking score value. Ligand interaction diagrams were generated using Schrödinger Maestro, ligand-receptor visualizations were generated using UCSF Chimera [43].

Acknowledgements

Authors sincerely acknowledge Prof. Budziszewska and Dr Bartosz Pomierny, Department of Toxicological Biochemistry, Jagiellonian University Medical College for enabling phospholipidosis tests evaluation on fluorescent microscopy DMi8 (Leica, Wetzlar, Germany). We are pleased to acknowledge the generous support of National Science Center, Poland granted on the basis of decision No. 2016/23/N/NZ7/00469, 2016/23/B/NZ7/01063, K/DSC/004310, and K/ZDS/007121. Support by DFG INST 208/664-1 (HS) and COST CA15135 (HS, KK) is also acknowledged.

Appendix A. Supplementary data

Supplementary data associated with this article can be found in the online version, at. These data include MOL files and InChiKeys of the most important compounds described in this article.

References

[1] Leurs R, Bakker RA, Timmerman H, de Esch IJP. The histamine H3 receptor: from gene cloning to H3 receptor drugs. *Nat Rev Drug Discov*. 2005; 4: 107–20.

[2] Gemkow MJ, Davenport AJ, Harich S, Ellenbroek BA, Cesura A, Hallett D. The histamine H3 receptor as a therapeutic drug target for CNS disorders. *Drug Discov Today*. 2009; 14: 509–15.

[3] Gao Z, Hurst WJ, Hall D, Hartung R, Reynolds W, Kang J, Nagorny R, Hendrix JA, George PG. Design and synthesis of a novel series of histamine H3 receptor antagonists through a scaffold hopping strategy. *Bioorg Med Chem*. 2014; 23: 429–38.

[4] Arrang JM, Garbarg M, Schwartz JC. Auto-inhibition of brain histamine-release mediated by a novel class (H3) of histamine receptor. *Nature*. 1983; 302: 832–7.

[5] Fox GB, Esbenshade TA, Pan JB, Radek RJ, Krueger KM, Yao BB, Browman KE, Buckley MJ, Ballard ME, Komater VA, Miner H, Zhang M, Faghih R, Rueter LE, Bitner RS, Drescher KU, Wetter J, Marsh K, Lemaire M, Porsolt RD, Bennani YL, Sullivan JP, Cowart MD, Decker MW, Hancock AA. Pharmacological properties of ABT-239 [4-(2-{2-[(2R)-2-Methylpyrrolidinyl]ethyl}-benzofuran-5-yl)benzonitrile]: II. Neurophysiological characterization and broad preclinical efficacy in cognition and schizophrenia of a potent and selective histamine H3 receptor antagonist. *J Pharmacol Exp Ther*. 2005; 313: 176–90.

[6] Passani MB, Blandina P. Histamine receptors in the CNS as targets for therapeutic intervention. *Trends Pharmacol Sci*. 2011; 32: 242–9.

[7] Schwartz JC. The histamine H3 receptor: From discovery to clinical trials with pitolisant. *Br J Pharmacol*. 2011; 163: 713–21.

[8] Bhowmik M, Khanam R, Vohora D. Histamine H3 receptor antagonists in relation to epilepsy and neurodegeneration: a systemic consideration of recent progress and perspectives. *Br J Pharmacol*. 2012; 167: 1398–414.

[9] Panula P, Chazot PL, Cowart M, Gutzmer R, Leurs R, Liu WL, Stark H, Thurmond RL, Haas HL. International Union of Basic and Clinical Pharmacology. XCVIII. Histamine Receptors. *Pharmacol Rev*. 2015; 67: 601–55.

[10] (a) Sadek B, Saad A, Sadeq A, Jalal F, Stark H. Histamine H_3 receptor as a potential target for cognitive symptoms in neuropsychiatric diseases. *Behav Brain Res*. 2016; 312: 415–430; (b) Bali A, Sharma K, Bhalla A, Bala S, Reddy D, Singh A, Kumar A. Synthesis, evaluation and computational studies on a series of acetophenone based 1-(aryloxypropyl)-4-(chloroaryl) piperazines as potential atypical antipsychotics. *Eur J Med Chem*. 2010; 45(6): 2656–62; (c) Faghih R, Dwight W, Gentles R, et al. Structure-activity relationships for non-imidazole H(3) receptor ligands. Part 1. Bioorg Med Chem Lett. 2002; 12: 2031–2034.

[11] Sadek B, Stark H. Cherry-picked ligands at histamine receptor subtypes. *Neuropharmacology*. 2016; 106: 56–73.

[12] Sadek B, Łażewska D, Hagenow S, Kieć-Kononowicz K, Stark H. Histamine H3R antagonists: from scaffold hopping to clinical candidates, in: Blandina P, Passani M (Eds.). Histamine Receptors. The Receptors vol. 28, Humana Press, Cham. 2016; https://doi.org/10.1007/978-3-319-40308-35.

[13] Stark H, Kathmann M, Schlicker E, Schunack W, Schlegel B, Sippl W. Medicinal chemical and pharmacological aspects of imidazole-containing histamine H_3 receptor antagonists. *Mini-Rev Med Chem*. 2004; 4: 965–977.

[14] Lacivita E, Leopoldo M, De Giorgio P, Berardi F, Perrone R. Determination of 1-aryl-4-propylpiperazine pKa values: the substituent on aryl modulates basicity. *Bioorg Med Chem*. 2009; 17: 1339–1344.

[15] Maia Rdo C, Tesch R, Fraga CA. Phenylpiperazine derivatives: a patent review (2006 – present). *Expert Opin Ther Patents*. 2012; 22 (10): 1169–1178.

[16] Szczepańska K, Karcz T, Mogilski S, Siwek A, Kuder KJ, Latacz G, Kubacka M, Hagenow S, Lubelska A, Olejarz A, Kotańska M, Sadek B, Stark H, Kieć-Kononowicz K. Synthesis and biological activity of novel *tert*-butyl and tert-pentylphenoxyalkyl piperazine derivatives as histamine H_3R ligands. *Eur J Med Chem*. 2018; 152: 223–234.

[17] Kotańska M, Kuder KJ, Szczepańska K, Sapa J, Kieć-Kononowicz K. The histamine H_3 receptor inverse agonist pitolisant reduces body weight in obese mice. *Naunyn-Schmiedeberg's Arch Pharmacol*. 2018; doi.org/10.1007/s00210-018-1516-2.

[18] Alter A. Disubstituted Piperazines Useful as Schistosomiasis Agents. 1966; US3270004.

[19] Kuder KJ, Łażewska D, Latacz G, Schwed JS, Karcz T, Stark H, Karolak-Wojciechowska J, Kieć-Kononowicz K. Chlorphenoxy aminoalkyl derivatives as histamine H_3R ligands and antiseizure agents. *Bioorg Med Chem*. 2016; 24: 53–72.

[20] Kottke T, Sander K, Weizel L, Schneider EH, Seifert S, Stark H. Receptorspecific functional efficacies of alkyl imidazoles as dual histamine H_3/H_4 receptor ligands. *Eur J Pharmacol*. 2011; 654: 200–208.

[21] Karlstedt K, Ahman MJ, Anichtchik OV, Soinila S, Panula P. Expression of the H3 receptor in the developing CNS and brown fat suggests novel roles for histamine. *Mol Cell Neurosci*. 2003; 24(3): 614–622.

[22] Nakamura T, Yoshikawa T, Noguchi N, Sugawara A, Kasajima A, Sasano H, Yanai K. The expression and function of histamine H_3 receptors in pancreatic beta cells. *Br J Pharmacol*. 2014; 171(1): 171–185.

[23] Dudek M, Marcinkowska M, Bucki A, Olczyk A, Kołaczkowski M. Idalopirdine - a small molecule antagonist of 5-HT6 with therapeutic potential against obesity. *Metab Brain Dis*. 2015; 30(6): 1487–1494.

[24] Cruciani G, Carosati E, De Boeck E, Ethirajulu K, Mackie C, Howe T, Vianello R. MetaSite: understanding metabolism in human cytochromes from the perspective of the chemist. *J Med Chem*. 2005; 48 (22): 6970–6979.

[25] Hancock AA. The challenge of drug discovery of a GPCR target: analysis of preclinical pharmacology of histamine H3 antagonists/inverse agonists. *Biochem Pharmacol*. 2006; 71: 1103–1113.

[26] Shimamura T, Shiroishi M, Weyand M, Tsujimoto H, Winter G, Katritch V, Abagyan R, Cherezov V, Liu W, Han GW, Kobayashi T, Stevens RC. Structure of the human histamine H1 receptor complex with doxepin. *Nature*. 2011; 475: 65–70.

[27] Ballesteros JA, Weinstein H. Integrated methods for the construction of three-dimensional models and computational probing of structure-function relations in G protein-coupled receptors. *Meth Neurosci*. 1995; 25: 366–428.

[28] Trzaskowski B, Latek D, Yuan S, Ghoshdastider U, Debinski A, Filipek S. Action of molecular switches in GPCRs -theoretical and experimental studies. *Curr Med Chem*. 2012; 19: 1090–1109.

[29] Cheng Y, Prusoff WH. Relationship between the inhibition constant (Ki) and the concentration of inhibitor which causes 50 per cent inhibition (I50) of an enzymatic reaction. *Biochem Pharmacol*. 1973; 22: 3099–3108.

[30] Dudek M, Kuder KJ, Kołaczkowski M, Olczyk A, Żmudzka E, Rak A, Bednarski M, Pytka K, Sapa J, Kieć-Kononowicz K. H_3 histamine receptor antagonist pitolisant reverses some subchronic disturbances induced by olanzapine in mice. *Metab Brain Dis*. 2016; 31: 1023–29.

[31] Kotańska M, Śniecikowska J, Jastrzębska-Więsek M, Kołaczkowski M, Pytka K. Metabolic and cardiovascular benefits and risks of EMD386088-A 5-HT_6 receptor partial agonist and dopamine transporter inhibitor. *Front Neurosci*. 2017; 11: 50.

[32] GraphPad Software, La Jolla California USA, www.graphpad.com.

[33] Latacz G, Lubelska A, Jastrzębska-Więsek M, Partyka A, Sobiło A, Olejarz A, Kucwaj-Brysz K, Satała G, Bojarski AJ, Wesołowska A, Kieć-Kononowicz K, Handzlik J. In the search for a lead structure among series of potent and selective hydantoin 5- HT7R agents: The drug- likeness *in vitro* study. *Chem Biol Drug Des*. 2017; 90 (6): 1295–1306.

[34] Latacz G, Lubelska A, Jastrzębska- Więsek M, Partyka A, Kucwaj-Brysz K, Wesołowska A, Kieć-Kononowicz K, Handzlik J. MF-8, a novel promising arylpiperazine-hydantoin based 5-HT7receptor antagonist: *In vitro* drug-likeness studies and *in vivo* pharmacological evaluation. *Bioorg Med Chem Lett*. 2018; 28 (5): 878–883.

[35] Schrödinger Release 2018-1, Schrödinger Suite 2018-1 Protein Preparation Wizard; Epik, Schrödinger, LLC, New York, NY; 2018.

[36] Sander K, Kottke T, Weizel L, Stark H. Kojic acid derivatives as histamine H(3) receptor ligands. *Chem Pharm Bull* (Tokyo). 2010; 58: 1353–1361.

[37] Sadek B, Kuder KJ, Subramanian D, Shafiullah M, Stark H, Łażewska D, Adem A, Kieć-Kononowicz K. Anticonvulsive effect of nonimidazole histamine H_3 receptor antagonists. *Behav Pharmacol*. 2014; 25: 245–252.

[38] Schrödinger Release 2018-1, ConfGen, Schrödinger, LLC, New York, NY; 2018.

[39] Watts KS, Dalal P, Murphy RB, Sherman W, Friesner RA, Shelley JC. ConfGen: a conformational search method for efficient generation of bioactive conformers. *J Chem Inf Model*. 2010; 50 (4): 534–546.

[40] Schrödinger Release 2018-1, Glide, Schrödinger, LLC, New York, NY; 2018.

[41] Halgren TA, Murphy RB, Friesner RA, Beard HS, Frye LL, Pollard WT, Banks JL. Glide: a new approach for rapid, accurate docking and scoring. 2. Enrichment factors in database screening. *J Med Chem*. 2004; 47 (7): 1750–1759.

[42] Friesner RA, Murphy RB, Repasky MP, Frye LL, Greenwood JR, Halgren TA, Sanschagrin PC, Mainz DT. Extra precision glide: docking and scoring incorporating a model of hydrophobic enclosure for Protein–Ligand complexes. *J Med Chem*. 2006; 49 (21): 6177–6196.

[43] Pettersen EF, Goddard TD, Huang CC, Couch GS, Greenblatt DM, Meng EC, Ferrin TE. UCSF Chimera – a visualization system for exploratory research and analysis. *J Comput Chem*. 2004; 25: 1605–1612.

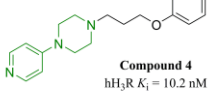

Compound 4
hH_3R K_i = 10.2 nM